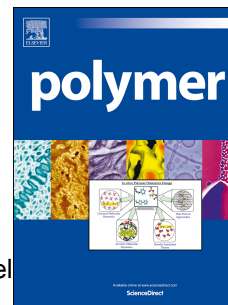


Journal Pre-proof

Structural, Thermal, and Mechanical properties of gelatin-based films integrated with tara gum

Luca Nuvoli, Paola Conte, Costantino Fadda, José Antonio Reglero Ruiz, José Miguel García Pérez, Salvatore Baldino, Alberto Mannu



PII: S0032-3861(20)31069-7

DOI: <https://doi.org/10.1016/j.polymer.2020.123244>

Reference: JPOL 123244

To appear in: *Polymer*

Received Date: 16 July 2020

Revised Date: 13 October 2020

Accepted Date: 16 November 2020

Please cite this article as: Nuvoli L, Conte P, Fadda C, Reglero Ruiz JA, García Pérez JM, Baldino S, Mannu A, Structural, Thermal, and Mechanical properties of gelatin-based films integrated with tara gum, *Polymer*, <https://doi.org/10.1016/j.polymer.2020.123244>.

This is a PDF file of an article that has undergone enhancements after acceptance, such as the addition of a cover page and metadata, and formatting for readability, but it is not yet the definitive version of record. This version will undergo additional copyediting, typesetting and review before it is published in its final form, but we are providing this version to give early visibility of the article. Please note that, during the production process, errors may be discovered which could affect the content, and all legal disclaimers that apply to the journal pertain.

© 2020 Elsevier Ltd. All rights reserved.

Structural, Thermal, and Mechanical properties of gelatin-based films integrated with tara gum

Luca Nuvoli,^a Paola Conte,^b Costantino Fadda,^b José Antonio Reglero Ruiz,^c
José Miguel García Pérez,^c Salvatore Baldino^d and Alberto Mannu^{d*}

^a Department of Chemistry and Pharmacy, University of Sassari and INSTM, Via Vienna 2, 07100 Sassari, Italy.

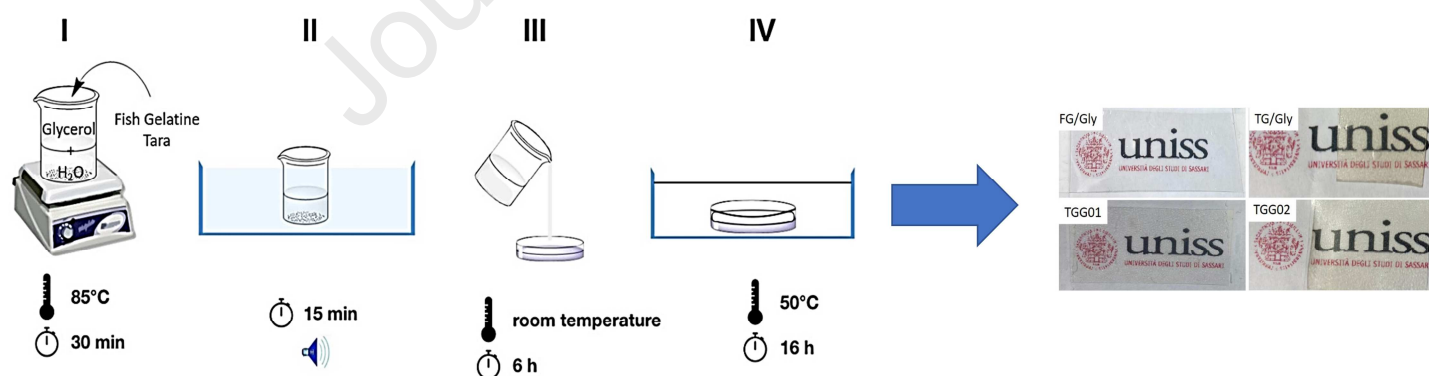
^b Department of Agriculture, University of Sassari, Viale Italia 39/A, 07100 Sassari, Italy.

^c Departamento de Química, Facultad de Ciencias, Universidad de Burgos, Plaza de Misael Bañuelos s/n, 09001 Burgos, Spain.

^d Dipartimento di Chimica, Università di Torino, Via Pietro Giuria, 7, I-10125 Torino, Italy.

*Corresponding author e-mail: alberto.mannu@unito.it

Easy fabrication process of Fish gelatin/tara films with high thermal stability



1 **Structural, Thermal, and Mechanical properties of gelatin-based films**
2 **integrated with tara gum**

3
4 Luca Nuvoli,^a Paola Conte,^b Costantino Fadda,^b José Antonio Reglero Ruiz,^c José Miguel
5 García Pérez,^c Salvatore Baldino^d and Alberto Mannu^{d*}

6 ^a Department of Chemistry and Pharmacy, University of Sassari and INSTM, Via Vienna 2,
7 07100 Sassari, Italy.

8 ^b Department of Agriculture, University of Sassari, Viale Italia 39/A, 07100 Sassari, Italy.

9 ^c Departamento de Química, Facultad de Ciencias, Universidad de Burgos, Plaza de
10 Misael

11 Bañuelos s/n, 09001 Burgos, Spain.

12 ^d Dipartimento di Chimica, Università di Torino, Via Pietro Giuria, 7, I-10125 Torino, Italy.

13
14 *Corresponding author e-mail: alberto.mannu@unito.it
15

Abstract

Films with different morphology can be obtained by mixing fish gelatin, Tara gum and glycerol in different ratio and by subjecting the Tara gum to a ball milling treatment before its use. The amount of the plasticizer glycerol, as well as the type of Tara gum employed (as received or milled) resulted, from SEM and AFM analyses, to strongly influencing the morphology of the films and their density. Also, the morphological differences determine different thermal and mechanical behaviours. In particular, the employment of milled Tara gum allows to improve the thermal stability, as well as the mechanical properties of the polymers. A similar outcome can be obtained by increasing the glycerol content, which can be used up to 20 wt%. Glycerol amounts exceeding that percentage, are detrimental for the quality of the films and reduce their thermal and mechanical performances.

Keywords: Tara gum; gelatin fish; biofilms

1. Introduction

During the last years, fervent research activities have been conducted on the engineering of composite gels. The possibility to tune gel properties combining specific components has gained increasing importance in many application fields, including food, drug delivery, tissue engineering and wound dressing [1,2,3].

Among the several components usually employed for composite gels engineering, gelatin, a mix of denaturated proteins derived by collagen [4,5,6], have attracted particular interest for biomedical and food packaging sectors, due its remarkable properties. As a matter of fact, gelatin is biocompatible, biodegradable, shows high capacity of cell adhesion and migration [7], shows antimicrobial properties [8], and it has been successfully exploited for tissue engineering [9,10]. Thermal properties of gelatin have been characterized in different papers. For example, Rahman *et al.* [11] presented a complete study about the glass transition and melting points of commercial mammalian gelatin, tuna gelatin, bovine gelatin and porcine gelatin. Glass transitions temperatures varied from 23 to 75 °C, whereas melting points were measured between 115 and 190 °C. These wide range of values, combined to their biocompatibility, make them suitable in many different biomedical applications, such as drug delivery or tissue engineering [12,13]. Of particular interest, especially for the packaging and biomedical sectors, are the Fish Gelatin (FG) based films. FG is cheap, biodegradable and easy to process for making films. In addition, its mechanical and optical properties can be modulated by adding polyols which act as

50 plasticizers. The main role of such additives consists in the denaturation of the FG's
51 proteins by reducing the interactions between protein chains and modifying the secondary,
52 tertiary and quaternary structures [14]. Within the polyols commonly employed for such
53 purpose, glycerol stands out as the ideal candidate. It showed good ability to interact with
54 FG, eco-compatibility, and it is available in large amount as by-product of waste vegetable
55 oils treatment [15], e.g. from biodiesel production [16]. On the other hand, the use of fish
56 gelatin in composite films is still limited by several factors such as low stability, poor
57 mechanical strength and low elasticity [17]. Many studies have been then conducted with
58 the aim to solve these weaknesses by exploring the doping with different additives
59 including synthetic and biological polymers [18].

60 Although different studies have been performed on the use of FG in composites in
61 combination with various additives, the interaction between gelatin and different natural
62 gums in modifying the thermal and mechanical properties of gelatin has been only recently
63 explored [19]. Natural gums have shown to allow structural engineering of thin films while
64 guaranteeing the biodegradability and edibility of the material [20]. Specific combinations
65 between natural gelatin, glycerol and natural gums have found important application
66 especially in food packaging [18].

67 Regarding the most employed natural gums (Tara, guar, and locust bean), Tara gum (Ta)
68 shows intermediate water solubility with respect to guar (cold soluble) and locust bean
69 gum (cold insoluble), making it ideal e.g. as food hydrocolloid [20]. Tara gum is obtained
70 by grinding the endosperm of the seeds of *Caesalpinia spinosa* (Fam. Leguminosae) and
71 it is composed by polysaccharide chains of high molecular weight based on the
72 galactomannan unit (See **Scheme S1** of the Electronic Supplementary Information file,
73 **ESI**). It has been approved as food additive due to its non-toxicity and thus it has gained
74 value as film additive [21]. When employed in gel composites, tara gum acts as thickening
75 agent and stabilizer.

76 In this context, herein, the fabrication and characterization of novel films based on fish
77 gelatin (FG), Tara gum (Ta), and glycerol (Gly), is reported. Ten films containing different
78 ratio of FG/Ta, different glycerol content and different types of Ta, are described and
79 characterized. For each film the structural, thermal, and mechanical properties are
80 discussed by means of, respectively, IR, X-ray, and SEM, Thermogravimetry (TG) and
81 differential scanning Calorimetry (DSC), and tensile properties analyses.

82

83 **2. Materials**

84 Tara gum (Aglumix 01, particle size 149 μm) and Fish Gelatin (LapiFish, particle size 2380
85 μm) were purchased, respectively, from Silvateam Food Ingredients S.r.l. and Lapi gelatin
86 S.p.a.. Fish gelatin with the following characteristics was employed: Bloom 280, mesh size
87 8-70, protein amount between 85% and 90%, water content 10-12%, and salts content 1-
88 2% [22].

89 Glycerol (90%) was purchased from Analyticals Carlo Erba, while acetone (>99%) and
90 ethanol (>99.5%) from VWR. All chemicals were used as received without any further
91 purification.

92

93 **3. Experimental equipment and methods**

94 Fourier transform infrared (FTIR) analysis was performed using a Bruker infrared Vertex
95 70 interferometer. The spectra were recorded on the films in transmission mode, in the
96 400-4000 cm^{-1} range by averaging 64 scans with 4 cm^{-1} of resolution.

97 Principal Component Analysis (PCA) as well as Partial Least Squares Discriminant
98 Analysis (PLS-DA) were conducted using of the tool Metaboanalyst 4 [23]. The spectral
99 data were centered and auto-scaled before the PCA and PLS-DA analysis.

100 The XRD patterns were collected using a Rigaku SmartLab X-ray powder diffractometer
101 aligned according to a Bragg–Brentano geometry with Cu K α radiation ($\lambda = 1.54178 \text{ \AA}$) and
102 equipped with a graphite monochromator in the diffracted beam. Since the polymers
103 showed broad haloes typical of amorphous condition, it was deliberately assumed to
104 restrict the reciprocal space investigation in the angular range from 5° to 80° in 2 θ , which
105 allows to determine the main shape features of specimen. Powders have been deposited
106 in an amorphous glass sample holder for measurements.

107 Ball milling of the Ta powders (15 g) was carried out in a SPEX Mixer/Mill 8000 at a
108 rotation speed of 875 rpm during 1 h, using two zirconia balls of 2 g each one. Taking in
109 consideration the very low amount of powders which are usually trapped (1 mg) at each
110 impact, and the stochastic nature of the ball milling process, over 200k collisions, occurring
111 under the mechanochemical conditions above reported, should be enough for refining
112 homogeneously all the batch powders [24]. Then, two different Tara gum powders were
113 obtained: as received (or non-milled) and milled.

114 The morphologies of the powders and films were observed by different techniques. First,
115 SEM images were taken using a FEI Quanta 200 scanning electron microscope. The
116 samples were placed on a double-sided carbon tape and examined at an acceleration
117 voltage of 20 kV under high vacuum. Also, Atomic Force Microscopy (AFM) images were

118 taken at RT using a confocal AFM-RAMAN model Alpha300R – Alpha300A from WITec,
119 using an AFM tip of 42 N/m.

120 The thermogravimetric analysis data were recorded on a TA Instrument Q50 TGA
121 analyzer. TGA tests were performed under O₂ (synthetic air) atmosphere using the next
122 procedure: first, samples were heated from RT to 100 °C at 10 °C/min, and then kept
123 during 10 min to eliminate the moisture content. Then, samples were heated up to 800 °C
124 at 10 °C/min.

125 DSC analyses were performed using a DSC Q200 TA Instruments equipment. Samples
126 were tested using a four-cycle procedure [25]. In the first cycle, after 5 min of stabilization
127 at RT, samples were heated up to 150 °C at 10 °C/min and then stabilized during 5 min
128 before cooling down in the second cycle to 30 °C at 20 °C/min. In the third cycle, samples
129 were heated up to 150 °C at 10 °C/min and after 5 min of stabilization at 150 °C, the fourth
130 cycle was performed: samples were cooled down to 30 °C at 20 °C/min. All the tests were
131 performed under N₂ atmosphere (flow rate 50 ml/min). Mass of the samples was fixed at
132 approximately 20 mg in each test. Glass transition temperature (T_g) was determined in the
133 third cycle.

134 To determine the tensile properties of the films, strips of 5 mm in width and 35 mm in
135 length were cut from each film. Tensile tests were carried out on a SHIMADZU EZ Test
136 Compact Table-Top Universal Tester at 20 °C. Mechanical clamps were used and an
137 extension rate of 5 mm/min was applied using a gauge length of 9.44 mm. At least 4 strips
138 were tested for each film in order to calculate the average value for each parameter
139 determined.

140

141 4. Preparation of films

142 The preparation of gelatin-based films is here detailed and schematized in **Figure S1** of
143 the **ESI**. Tara powder was added to a solution of glycerol and distilled water and the
144 mixture was stirred at 85°C during 30 minutes until a homogeneity was reached (**I**). Then,
145 Fish gelatin was added at 85 °C and stirred until dissolution (**II**). The mixture was
146 subjected to ultrasound for 15 minutes to remove air bubbles (**III**). Film-forming solutions
147 were poured into Steriplan® petri dished (80 mm x 15 mm) and dried at room temperature
148 for 6 h and then located at 50 °C in humidity-controlled oven for 16 hours (**IV**). The
149 corresponding film was thoroughly washed with ethanol and acetone to afford the desired
150 gel.

151

5. Results and discussion

5.1 Density and visual aspect of the films

Ten films composed by Fish gelatin (FG), Tara powder (Ta) and glycerol (Gly) were prepared with different Ta/FG ratio (1/2, 1/1, and 2/1) and Gly amount (20, 40, and 60 wt%). Additionally, two reference films (FG/Gly and Ta/Gly) were also prepared to compare their properties with the FG/Ta/Gly films. Finally, two types of Ta were considered: as received by the purchaser, and milled. Nomenclature, density and composition of the films fabricated are reported in **Table 1**.

Table 1. Nomenclature, density and composition of the films fabricated.

Film	FG (eq. wt.)	Ta (eq. wt.)	Ball Milling	Gly (wt%)	Density (g/cm ³)
TGG01	1	1	No	20	7.9
TGG02	1	1	Yes	20	8.6
TGG03	1	1	No	40	6.8
TGG04	1	1	Yes	40	8.2
TGG05	1	1	No	60	6.5
TGG06	1	1	Yes	60	7.2
TGG07	2	1	No	20	7.8
TGG08	2	1	Yes	20	8.7
TGG09	1	2	No	20	9.1
TGG10	1	2	Yes	20	9.8
FG/Gly	1	0	No	20	4.7
Ta/Gly	0	1	No	20	10.0

Table 1 shows that densities obtained vary from 6.5 g/cm³ for TGG05 film to 9.8 g/cm³ for TGG10 film. Also, it can be noticed that the density of the as-casted films increases for systems containing milled Tara powder compared to those produced using the non-milled one (TGG02 vs TGG01). A relevant influence glycerol content on the density values was observed, which decrease at higher wt% of glycerol (TGG06 vs TGG02). As expected, pure FG film shows the lower density value (4.7 g/cm³), while pure Tara film presents the higher density value (10.0 g/cm³).

From a qualitative visual analysis, film specimens were transparent despite Ta/Gly presented a slightly yellow to brown appearance with respect to FG/Gly film. On the other hand, in TGG01 to TGG10 films opaqueness is reduced. This means that opacity could be

174 related to the Tara adding effect and its dispersion during film preparation, causing the
 175 reduction of the film transparency with respect to starting Fish gelatin film. This
 176 characteristic could limit the use of films composed by only Tara in food packaging
 177 applications. In **Figure 1** the photographs of the films FG/Gly, Ta/Gly, TGG01 and TGG02
 178 are shown.

179

180

181

182

183

184

185

186



187

Figure 1. Photographs of the FG/Gly, Ta/Gly, TGG01 and TGG02 films.

188

189

5.2 FT-IR analysis

190

191

192

193

194

195

196

197

198

199

200

201

202

203

204

205

206

207

A first quality check on the effect of the preparation procedure on the chemical composition of the constituents of films TGG01-TGG10 was performed by FTIR analysis. Results are displayed in **Figure S2** of the **ESI**. The absorption bands for gelatin-based composite films in the IR spectra are situated in the amide band region. The band situated around 3299, 1635, 1550, 1238 cm^{-1} correspond to amide-A (NH-stretching coupled with hydrogen bonding) and water molecules, amide I (C=O stretching/hydrogen bonding coupled with COO), amide II (bending vibration of N-H groups and stretching vibrations of C-N groups), and amide III (vibrations in the plane of C-N and N-H groups of bound amid). The bands in the FTIR spectrum of Tara powder appear in two major regions, 3700-2500 cm^{-1} and 1700-700 cm^{-1} . The broad band at 3700-3000 cm^{-1} is a result of O-H stretching vibration which is associated with free, inter and intra-molecular bonded hydroxyl groups. The shoulder-shaped band at about 2920 cm^{-1} is the stretching vibration of $-\text{CH}_2$. The bands at 1020 cm^{-1} is characteristic of the O-C stretching vibration of the anhydro glucose ring. These bands indicate that Tara powder has the general properties of a polysaccharide [26, **Error! Bookmark not defined.**].

If from one side the FT-IR data confirm the expected composition of the films, ruling out any thermal decomposition which can occur during the synthesis from the other side, [27, **Error! Bookmark not defined.**] by a visual analysis of the plots reported in **Figure S2**,

208 few information can be obtained on the differences between films with different
209 composition [28,29].

210 In order to analyse better the available FT-IR data and to extrapolate as more information
211 as possible, a multivariate analysis of the spectral data was conducted. The normalized
212 frequencies relative to films TGG01-TGG10 were considered for building a spectral
213 fingerprint of each film. The aim of such statistical analysis was to distinguish between
214 films containing milled and not-milled Tara. At first, non-supervised Principal Component
215 Analysis (PCA) was conducted, as shown in **Figure S3** of the **ESI**.

216 As expected, PCA analysis of the FT-IR intensities doesn't allow to reach a perfect
217 discrimination. In fact, unbiased PCA method works properly when within-group variation,
218 [30] in this case related with FG/Ta ratio and glycerol content, is sufficiently less than
219 between-group variation (milled and not-milled Tara). Nevertheless, a supervised
220 approach as the Partial Least Squares Discriminant Analysis (PLS-DA) can be used for
221 classify the two considered groups and discuss properly differences between films, as it is
222 presented in **Figure S4** of the **ESI**, in which 2D Component 1 vs Component 2 Plot of FT-
223 IR intensities of films TGG01-TGG10, containing milled (M) and not-milled (NM) Ta are
224 shown.

225 From the information of **Figure S4** it is possible to appreciate the discrimination between
226 films contained milled and not-milled Ta obtained through multivariate PLS-DA analysis.
227 The analysis, even qualitative, of the distances between the labels in the Scores Plot is of
228 particular interest. Comparing films containing milled (M) and not-milled (NM) Tara, it is
229 possible to notice incremental differences following the trend TGG03-TGG04, TGG05-
230 TGG06, TGG07-TGG08, and TGG09-TGG10, indicating an increasing effect of the Ta
231 grain size which depend on the amount of glycerol and on the FG/Ta ratio. More glycerol is
232 present, more the milled Tara is distinguishable from the not-milled one (TGG02, TGG04,
233 TGG06 vs TGG03, TGG05, and TGG07). As matter of fact, films containing an FG/Ta ratio
234 of 1/2 or 2/1 seems to be more sensitive to the type of Tara (TGG08, TGG10 vs TGG09,
235 and TGG10). FT-IR qualitative analysis highlighted important chemical differences within
236 films with different glycerol content and Tara typology. If the effect of the plasticizer
237 (glycerol) it is known and expected, the possibility to affect the composition of a film by
238 changing the granulometry of the Tara deserves more attention.

239

240 **5.3 X-ray diffraction analysis**

241 With the aim to better assess the structural differences between films TGG01-TGG10, X-
242 ray diffraction analysis was conducted. Figure **S5** of the **ESI** displays the XRD patterns of
243 all the films prepared. Ta presents a broad peak at $\sim 19^\circ$ indicating amorphous and
244 crystalline regions existed because a large amount of $-OH$ groups interacted via
245 intermolecular hydrogen bonds. This peak partially disappeared in the composite film,
246 indicating that a part of Tara molecules was in ordered arrangement, which was
247 interrupted in the grafting process; therefore, the obtained composite is amorphous. After
248 grafting, the peak strength decreased, which indicated that intermolecular hydrogen bonds
249 were damaged.

250 The diffractogram pattern acquired on the FG/Gly film was typical of a partially crystalline
251 gelatin with a sharp peak located at $2\theta = 7.1^\circ$ ($d_{101} = 12.29 \text{ \AA}$) and a broad peak located at
252 $2\theta = 20^\circ$ ($d_{101} = 4.09 \text{ \AA}$), as shown in **Figure S5**. These characteristic peaks are usually
253 assigned to the triple-helical crystalline structure in gelatin. In particular, the first diffraction
254 peak at 7° (sharp and intense) is directly related to the diameter of the triple helix. It was
255 also found that the addition of polyols such as glycerol most often decreases the intensity
256 of the first peak ($2\theta = 7^\circ$). Furthermore, it has been observed that the addition of tara gum
257 shifted the diffraction angle from 7.1° to 9.12° (for TGG05/06 and TGG09/10 films) then
258 decreasing the diameter of the inter reticular triple helix. On the other hand, this intensity of
259 peaks decreases and, in some cases, completely disappeared (TGG01/02, TGG03/04 and
260 TGG07/08 films). The disappearance of X-ray diffraction peaks corresponding to the
261 composites films confirms the interaction between two biopolymers. This phenomenon
262 illustrates the reduction hydrogen bonds between hydroxyls group of gelatin and those of
263 anhydroglucose of Tara gum, which limited the movement of molecules and thus
264 prevented crystallization.

265 The addition of glycerol seems to decrease the intensities of the gelatin peak making the
266 film more amorphous as compared to control gelatin film. This is probably due to the high
267 stability of these films when glycerol was added. Finally, a clear effect of BM was observed
268 only on TGG06 system which presented a significant decrease on the peak intensity at 2θ
269 $= 19.9^\circ$ with respect to TGG05. This effect could be related with the synergic effect of
270 glycerol addition and Tara gum added with refined particle size, and it confirms the
271 influence of Tara granulometry qualitatively observed by FT-IR.

272

273 **5.4 Morphological analysis**

274 An exhaustive morphology analysis of the films TGG01-TGG10 was conducted by different
275 approaches. Firstly, Scanning Electron Microscopy (SEM) images of the films were
276 collected as shown in **Figure 2**.

277

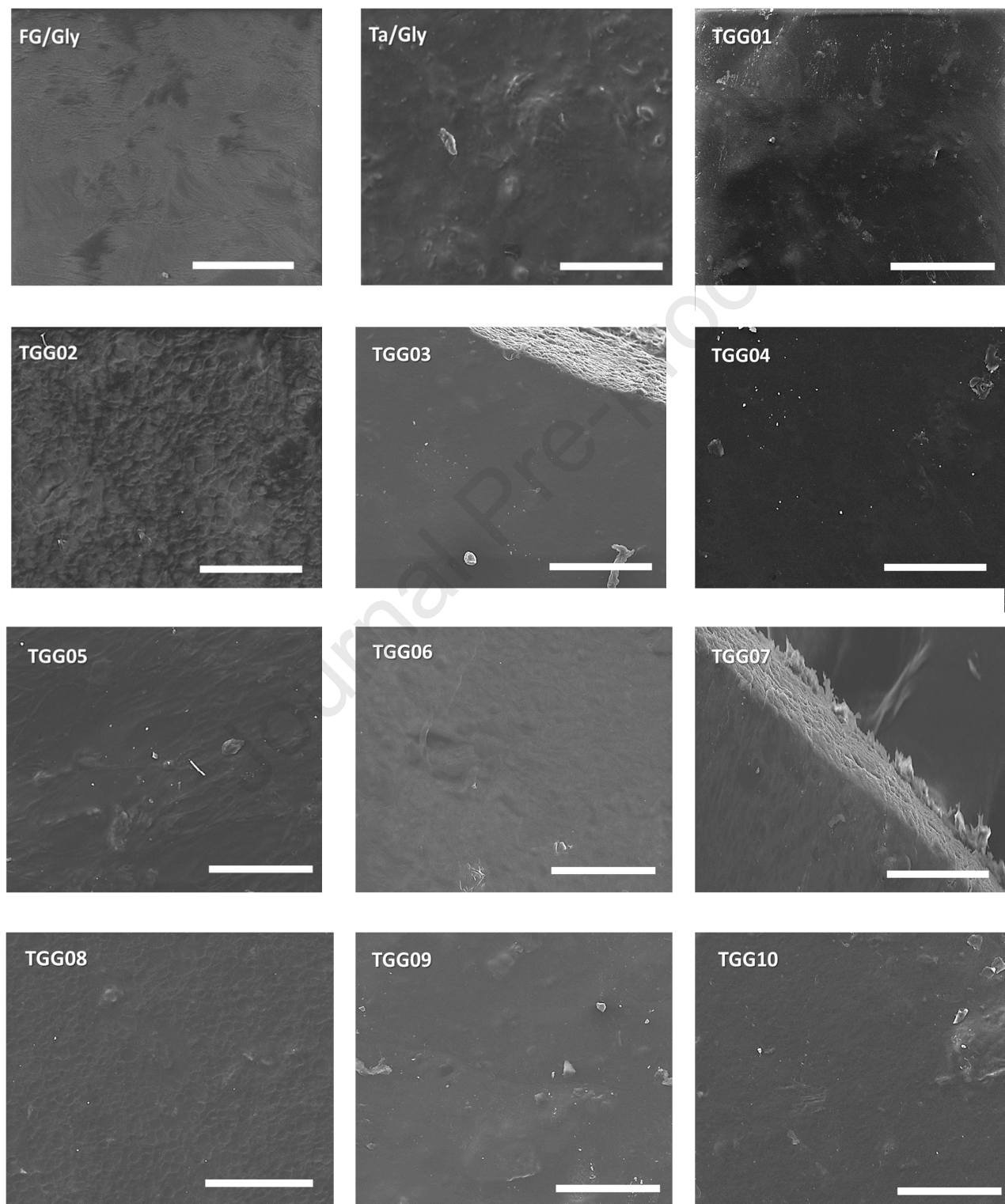


Figure 2. SEM images of the films prepared (bar scale 100 μm).

278

279 Micrographs in **Figure 2** show that surfaces of TGG films were homogeneous although
280 pores were observed on the top of each system, except in the case of FG/Gly film. In
281 addition, bigger and fewer pores were found in the TGG01, TG003, TGG05, TGG07 and
282 TG009 films, all of them fabricated using the un-milled Ta powder. On the other hand,
283 more and smaller uniform pores were observed on the surface of the TGG02, TG004,
284 TGG06, TG008 and TGG10 films, in which ball milled Tara powders were introduced.
285 Then, it is clear that this difference could be ascribable to the reduced Tara particles sizes
286 obtained upon ball milling.

287 **Figure 4** presents the AFM surface images of TGG09 and TGG10 films, in which the
288 distribution of Tara powder (non-milled in the case of TGG09 film and milled in the case of
289 TGG10) is observed. AFM surface images do not show great differences in the Tara
290 powder distribution, showing that, in general, Tara powder is well dispersed in the film
291 surface. Only a few agglomerated Tara particles are observed in the surface of the films,
292 as it can be seen in the yellow circles spotted of **Figures 4a** and **4c**.

293 The effect of the milling ball can be analyzed from two different points of view. First, it
294 seems that the size of the agglomerated particles is slightly higher when non milled Tara is
295 employed, as it can be seen in the agglomeration of Tara particles in **Figures 4a** (TGG09,
296 non-milled Tara) and **4c** (TGG10, milled Tara). Secondly, the size distribution of Tara
297 particles can be observed in the AFM surfaces images presented in **Figures 4b** (TGG09)
298 and **4d** (TGG10). In this case, there is not a very clear difference between the particles
299 size of non-milled (**Figure 4b**) and milled Tara (**Figure 4d**), but it can be detected that
300 milling the Tara powder could reduce the particle size compared to non-milled Tara. In this
301 sense, **Figure 4d** show Tara particles with sizes below 1 μm of diameter, and on the other
302 hand, **Figure 4b** presents, in the bottom-left zone, Tara particles with higher sizes (around
303 1 μm).

304

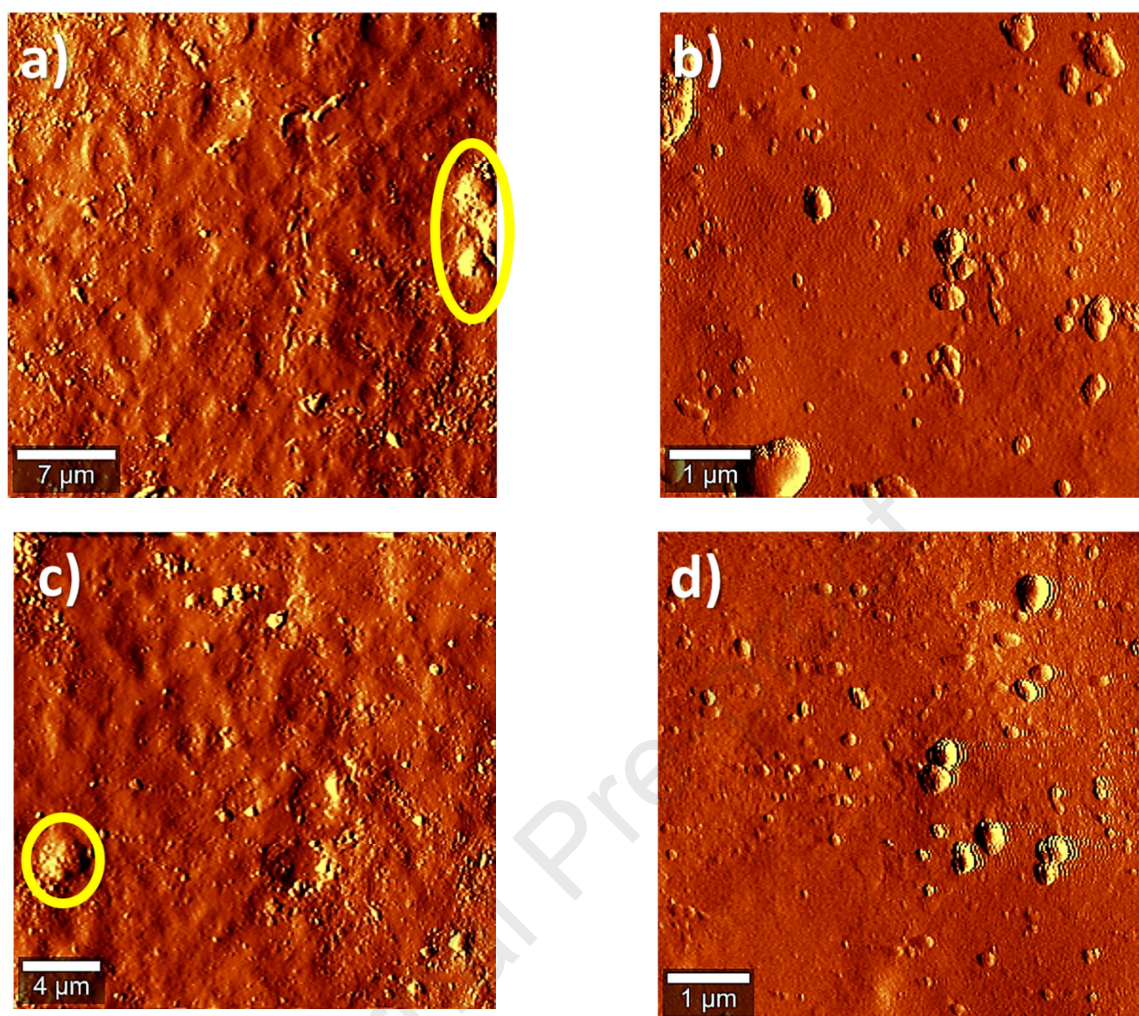


Figure 4. AFM surface images of TGG09 (a and b) and TGG10 (c and d) films.

305

306

5.5 Thermal stability of films

307

308

309

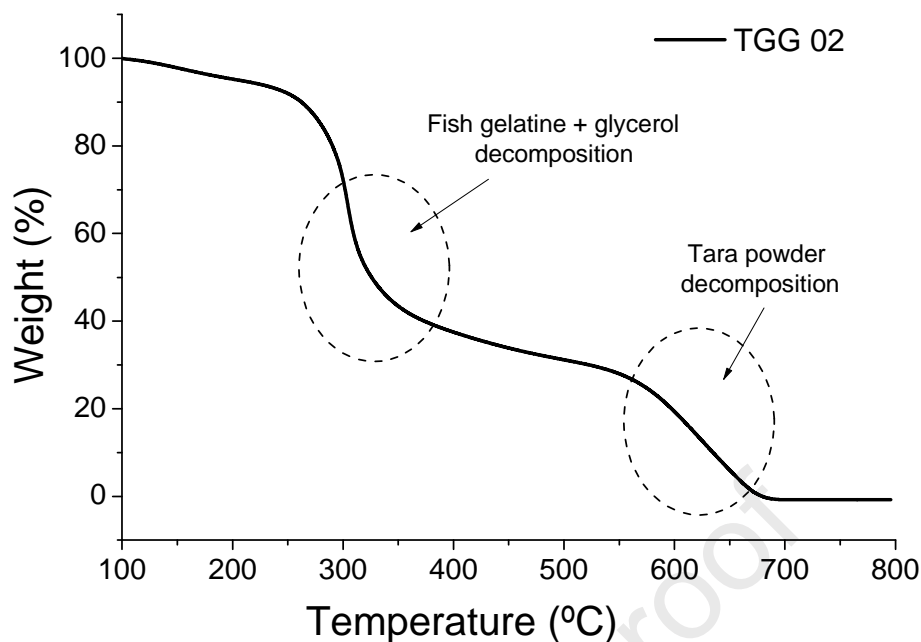
310

311

312

313

Preliminary structural and morphological analyses on films TGG01-TGG10 revealed a not negligible effect of Tara granulometry. Films with different structures should manifest different thermal and mechanical behavior. Regarding the thermal stability, it was assessed by TGA analysis. Information about the degradation and mode of decomposition under the effect of heat were also acquired. In **Figure 4**, the TGA thermogram of film TGG02 is presented as an example.



314

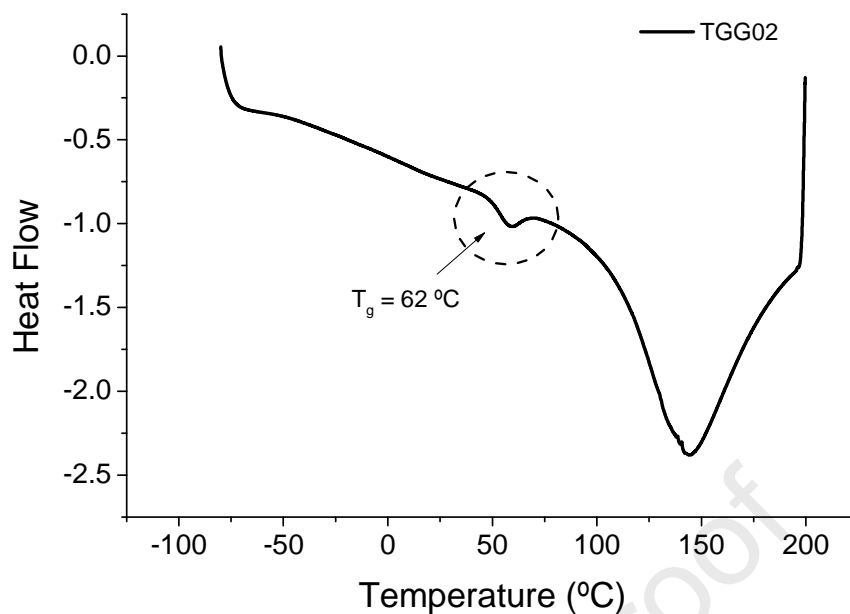
315 **Figure 4.** TGA profile of film TGG02.

316

317 From the thermogram presented in **Figure 4**, two weight losses are clearly detected.
318 Decomposition of fish gelatin-glycerol polymeric structure is detected around 300 °C,
319 whereas Tara powder degradation begins at 550 °C. The complete set of thermograms
320 obtained from all the films fabricated are presented in **Figure S6** of the **ESI**.

321 Additionally, Differential Scanning Calorimetry (DSC) analysis were performed on TGG01-
322 TGG10 films. The DSC measurements were employed for the determination of the glass
323 transition temperature (T_g), measured during the third cycle of the measurement
324 procedure. An example of the glass transition region is presented in **Figure 5**, in which the
325 DSC curve of the TGG02 film is showed, in which the T_g is appears around 62 °C. The
326 DSC curves obtained from all the films, in which the T_g region is observed, is shown in
327 **Figure S7** of the **ESI**.

328



329

330 **Figure 5.** DSC curve (third cycle) obtained for TGG02 film.

331

332 All the thermal data derived from TGA and DSC tests corresponding to all the films
 333 fabricated are reported in **Table 2**.

334

335 **Table 2.** Thermal properties of all the films prepared. T_g is the glass transition temperature,
 336 humidity loss percentage was measured directly as the quantity of mass loss at 100 °C, $T_{5\%}$ and
 337 $T_{10\%}$ are the temperatures at which 5 % and 10 % of mass is lost, and Onset temperature is
 338 defined as the temperature at which the decomposition of the material begins.

Film	T_g (°C)	Humidity loss (%)	$T_{5\%}$ (°C)	$T_{10\%}$ (°C)	Onset (°C)
TGG 01	63	9.8	213	245	274
TGG 02	62	6.9	224	268	294
TGG 03	52	10.7	190	218	266
TGG 04	54	10.1	193	237	287
TGG 05	50	10.5	175	207	259
TGG 06	51	7.3	244	261	275
TGG 07	69	9.7	207	244	274
TGG 08	61	8.1	215	251	277
TGG 09	63	6.1	217	263	287
TGG 10	58	5.3	228	268	293
FG/Gly	48	4.1	121	191	264
Ta/Gly	52	11.7	258	269	319

339

340 As it can be seen in data in **Table 2**, pure FG films (FG/Gly) present the lower $T_{5\%}$, $T_{10\%}$
341 and onset temperature values, with temperatures of 121 °C, 191 °C and 264 °C,
342 respectively. Comparing these data with the thermal behavior of pure Tara films (Ta/Gly),
343 values are considerably increased ($T_{5\%}$, $T_{10\%}$ and onset values are 258 °C, 269 °C and
344 319 °C), indicating that the Tara powder has a better thermal stability than Fish gelatin. In
345 both cases, the quantity of glycerol employed is 20 wt%.

346 Values of $T_{5\%}$, $T_{10\%}$ and onset temperature in Tara-gelatin films (TGG01 to TGG10) lie
347 between the limit values showed by the FG/Gly and Ta/Gly. In this sense, it is
348 demonstrated the good thermal behavior of composite films respect to pure FG film. This
349 improvement on the thermal behavior depends strongly on the quantity of glycerol, but we
350 can even remark that films with high glycerol content (TGG 05 and TGG 06, with 60 wt%
351 of glycerol) present a good thermal stability (onset temperatures are 259 °C and 275 °C).

352 As expected, the quantity of glycerol has a predominant effect in the thermal stability of the
353 films. In this sense, increasing the glycerol content lowers the $T_{5\%}$ and $T_{10\%}$ temperatures,
354 then affecting negatively to the thermal stability and to the processing or working
355 temperatures. On the other hand, using milled Tara seems to affect positively in the
356 thermal stability of the films. For example, comparing the TGA data of TGG 01 (non-milled
357 Tara) and TGG 02 (milled Tara), it can be seen that $T_{5\%}$, $T_{10\%}$ and onset temperatures are
358 increased up to 20 °C, indicating that the use of milled Tara also increases the thermal
359 stability of the films, obtaining films stable up to 300 °C, making them easy processable
360 [31]. Finally, the humidity content values for TGG films vary between the limit values
361 marked for pure Fish gelatin film (4.1 %) and pure Tara film (11.7 %). In this case, the use
362 of milled Tara reduces the humidity content respect to films with non-milled Tara
363 (compare, for example, humidity content values of TGG 01 and TGG 02 films). This is also
364 a very positive effect in terms of stability and handleability of the films. It is important to
365 remark that similar humidity loss and thermal decomposition profiles were reported by
366 Pulieri *et al.* in the case of Chitosan/gelatin blends [32].

367 Concerning the analysis of the glass transition temperature, it emerges that TGG films
368 show higher T_g values with respect to FG/Gly, although this difference is not very
369 important (in Ta/Gly film was not possible to measure the T_g temperature precisely). The
370 discussion of the results can be carried out taking into account three different separated
371 effects: (i) The influence of the Ta/FG ratio on the T_g , (ii) The effect of glycerol weight
372 percentage, and (iii), the type of Ta employed (milled or not milled).

373 **Figure 6** shows the T_g variation in all the films as a function of the Ta/FG ratio (**Figure 5a**)
 374 and also as a function of glycerol weight percentage (**Figure 5b**).

375

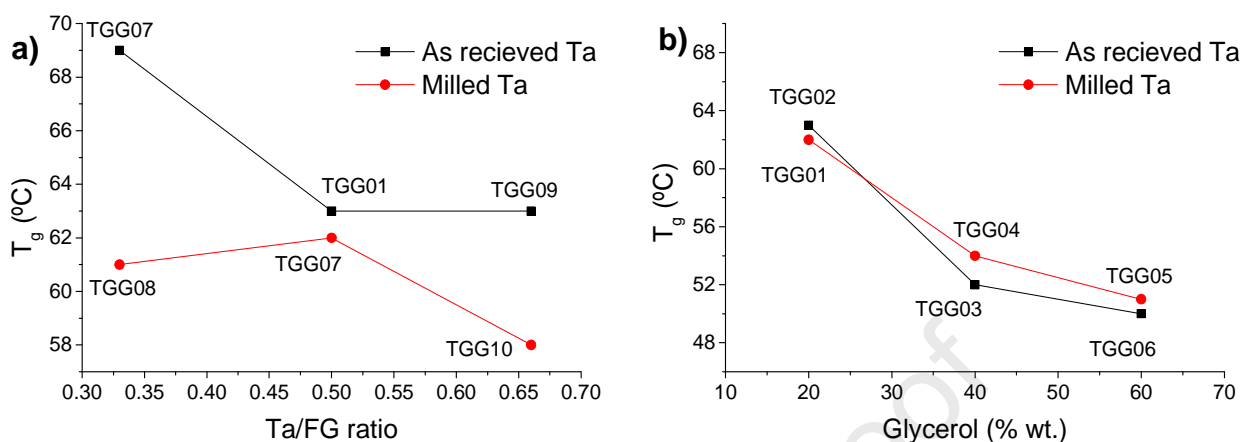


Figure 6. T_g values of films fabricated. a) Films with different Ta/FG ratio; b) Films with different glycerol weight percentage.

376

377 **Figure 6a** shows the influence of the Ta/FG ratio in the glass transition temperature.
 378 Having a look at films fabricated using non milled Tara, a reduction of T_g is observed when
 379 the Ta/FG ratio increases. On the other hand, the effect of the glycerol weight percentage
 380 is clearly observed (**Figure 6b**). As expected, the addition of glycerol decreases the T_g ,
 381 confirming the role of glycerol as plasticizer. Finally, the third effect is related to the Tara
 382 powder employed (non-milled or milled). The analysis of the data in **Figure 6** shows that
 383 using milled Tara increases the glass transition temperature, but only when TGG07 vs
 384 TGG08 and TGG09 vs TGG10 films are compared (see **Figure 6a**). In these particular
 385 cases, T_g is increased around 7 °C.

386

387

5.6 Tensile properties

388 To analyse the mechanical behaviour of films TGG01-TGG10, tensile properties were
 389 measured. Three different parameters were determined from the stress (σ)-strain (ϵ)
 390 curves: Young modulus E , stress (σ_{break} , (MPa)) and deformation at break (ϵ_{break} , (%)).

391 **Figure S8** of the **ESI** shows the stress-strain curves obtained for all the films fabricated,
 392 while **Table 3** presents the corresponding mechanical data.

393

394

395

396

397 **Table 3.** Mechanical data of the films TGG01-TGG10.

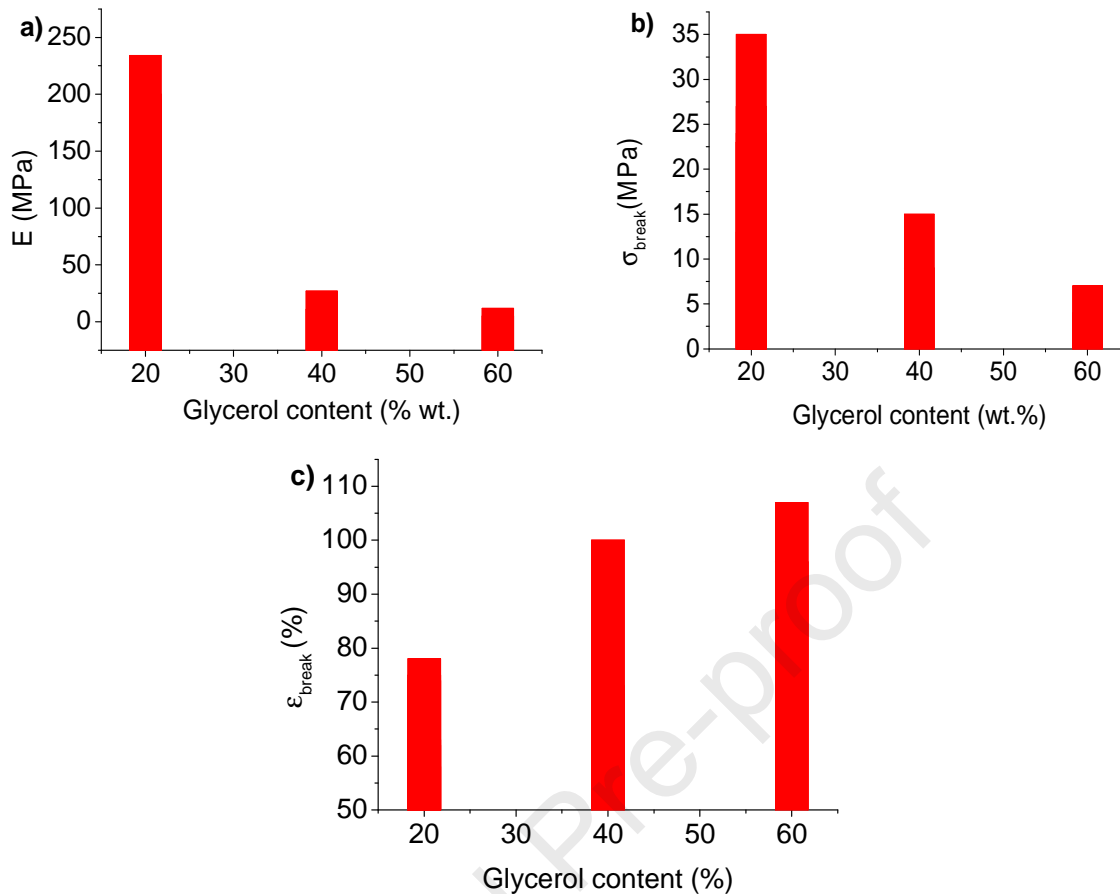
Film	E (MPa)	Δ^1 (MPa)	σ_{break} (MPa)	Δ^1 (MPa)	ϵ_{break} (%)	Δ^1 (%)
TGG 01	97	13.3	24	2.5	75	7.3
TGG 02	195	18.8	23	1.5	58	6.4
TGG 03	11	2.7	9	2.9	100	11.1
TGG 04	27	5.4	15	3.1	73	9.2
TGG 05	5	1.2	4	0.3	107	8.6
TGG 06	12	4.4	7	2.5	96	14.1
TGG 07	194	19.8	27	3.1	62	13.2
TGG 08	94	21.1	13	2.1	78	4.1
TGG 09	234	17.8	35	5.2	74	17.2
TGG 10	200	21.2	23	1.5	63	12.3
FG/Gly	243	5.9	36	3.8	95	6.1
Ta/Gly	550	31.7	40	13.2	23	7.0

398 ¹ Δ indicate the standard deviation of each value.

399

400 Mechanical data presented in **Table 3** indicate that Young's moduli values show a wide
 401 variability, from 5 MPa (TGG 05) to 234 MPa (TGG 09), as well as the stress at break,
 402 included between 4 MPa (TGG05) and 35 MPa (TGG09). Consequently, the deformation
 403 at break range between 23% and 107%.

404 This variability in the mechanical data can be related to the glycerol content and its
 405 plasticization effect, which plays a key role in the mechanical performance of the materials.
 406 In order to better highlight this effect, the dependence of the mechanical parameters with
 407 the glycerol content is reported in **Figure 7**.



408

409

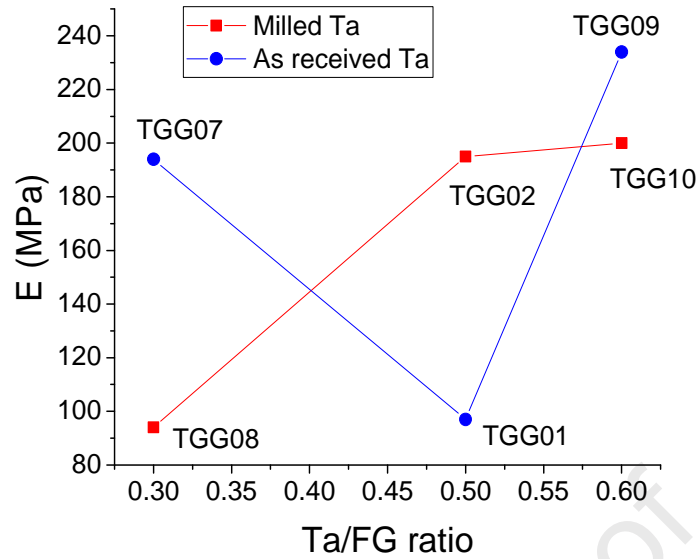
410 **Figure 7.** Dependence of the mechanical data of the films with glycerol content. a) Young's moduli,
 411 b) Stress at break, and c) Deformation at break.

412

413 It can be observed that the Young's moduli, as well as the stress at break decrease when
 414 glycerol is added, while the deformation at break increases with the content of glycerol.
 415 This behaviour confirms the plasticization effect expected through the addition of glycerol
 416 in the initial formulation of the materials.

417 Having a look at the values individually, TGG09 and TGG10 films present the higher
 418 values of Young's moduli (234 and 200 MPa). This is directly related to the Tara powder
 419 content, which is higher in these films (2 wt. eq).

420 In addition to the two main effects discussed above, a not-negligible influence of the Tara
 421 grain size on the mechanical properties can be observed. In **Figure 8**, the variation of E as
 422 function of Ta/FG ratio and type of Tara (milled and not milled) is reported.



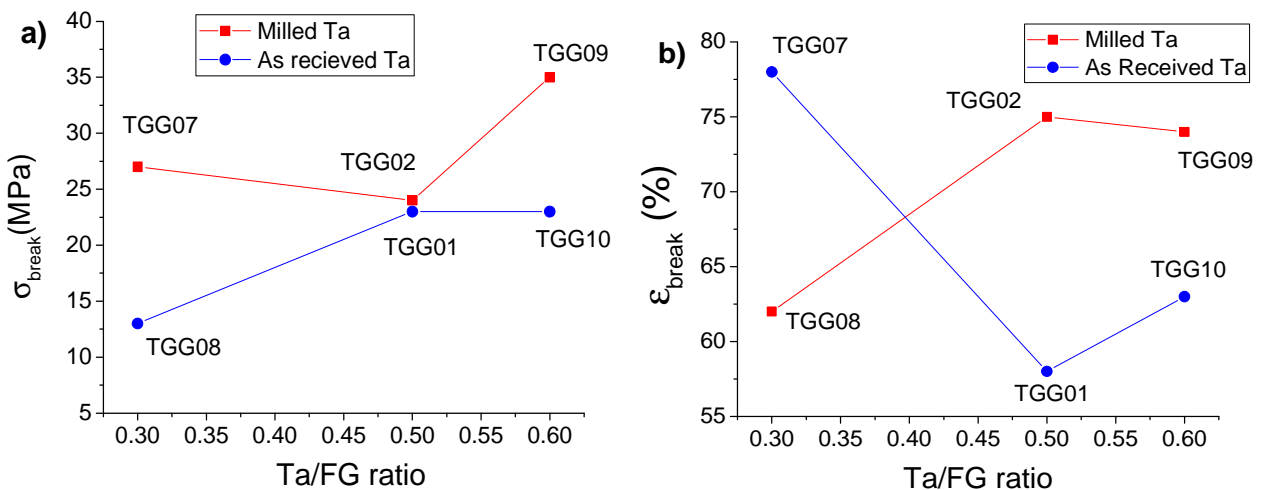
423

424 **Figure 8.** Variation of Young modulus E with the Ta/FG ratio and effect of the ball-milling of Tara
 425 gum powder.

426

427 From the plots showed in **Figure 8** it is possible to notice a different mechanical behaviour
 428 of films containing milled Ta which influences differently the trends of the two series
 429 TGG07-TGG01-TGG09 and TGG08-TGG02-TGG10 (**Figure 8**, circled and squared
 430 points). Films prepared with not milled Tara show a difference in Young's moduli value of
 431 about 100 MPa for Ta/FG $\frac{1}{2}$ ratio (TGG07 vs TGG08) and for Ta/FG ratio of 1/1 (TGG02
 432 vs TGG01), but with opposite trends. In the presence of an excess of Tara, the Young's
 433 moduli values are quite similar, with not milled films showing a value slightly higher.
 434 Finally, to better compare the curves relative to films containing non-milled and milled
 435 Tara, the variation of stress at break and deformation at break of films containing the two
 436 different Tara powders is reported in **Figure 9**.

437



438

439 **Figure 9.** Mechanical data as function of Ta/FG of films containing non-milled or milled Tara gum
440 powder. a) Stress at break; b) Deformation at break.

441

442 Data in **Figure 9** indicates that stress at brake is affected by the presence of milled Tara
443 only in films containing with Ta/FG ratio 2/1 or 1/2, while the mechanical values for Ta/FG
444 ratio of 1/1 are almost coincident (**Figure 9a**). On the contrary, the deformation at brake
445 shows a different behaviour depending of the Tara employed. When non-milled Tara is
446 used, deformation at break grows with the increasing of Tara content, whereas on the
447 other hand when milled Tara is employed the trend is the opposite (**Figure 9b**).

448

449 **6. Conclusions**

450 Morphological, thermal and mechanical properties of films composed by fish gelatin, Tara
451 gum and glycerol can be tuned by oportune engineering processes. In particular, by
452 changing the amount of the plasticizer glycerol, it is possible to optimize the composition in
453 terms of thermal behaviour and mechanical properties. Also, the structural effect obtained
454 by the addition of Tara gum resulted relevant. By employing milled Tara instead to the
455 commercial one, it is possible to enhance the thermal stability and improve the mechanical
456 performances of the films. The origin of such effects can be found in a change of the
457 morfology of films prepared with different ingredients, and observed by IR spectroscopy
458 and through SEM and AFM analyses. Influencing the performances of the films by
459 reducing the grain size of the natural gum (Tara in our case) represents a novelty and can
460 lead the way toward further optimization of similar polymers.

461

462 **Acknowledgments**

463 The financial support provided by FEDER (Fondo Europeo de Desarrollo Regional) and
464 both the Spanish Agencia Estatal de Investigación (MAT2017-84501-R) and the
465 Consejería de Educación, Junta de Castilla y León (BU306P18) is gratefully
466 acknowledged.

467

468 **Data Availability**

469 The raw data required to reproduce these findings cannot be shared at this time due to
470 technical limitations.

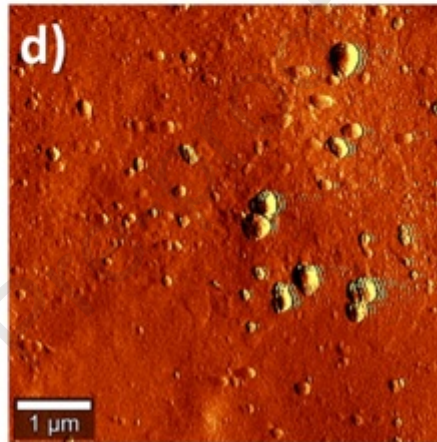
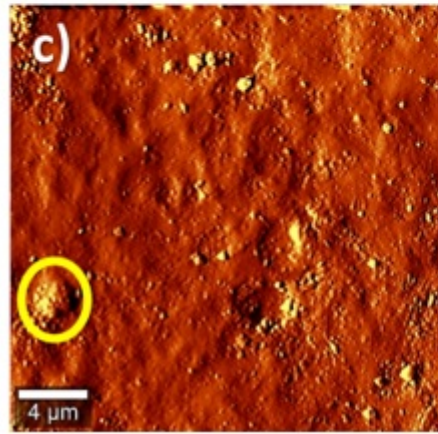
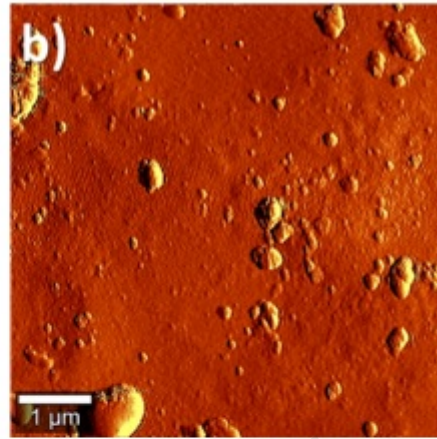
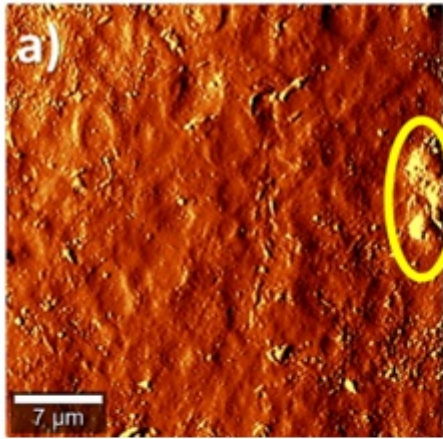
471

472 **References**

- [1] R. Rodríguez-Rodríguez, H. Espinosa-Andrews, C. Velasquillo-Martínez, Z. Y. García-Carvajal, Composite hydrogels based on gelatin, chitosan and polyvinyl alcohol to biomedical applications: a review, *Int. J. Polym. Mater.* 69 (2015) 1-20. <https://doi.org/10.1080/00914037.2019.1581780>.
- [2] T. Huang, Z. Fang, H. Zhao, D. Xu, W. Yang, W. Yu, J. Zhang, Physical properties and release kinetics of electron beam irradiated fish gelatin films with antioxidants of bamboo leaves, *Food Bioscience*, 36 (2020), 100597. <https://doi.org/10.1016/j.fbio.2020.100597>.
- [3] T. Huang, J. Lin, Z. Fang, W. Yu, Z. Li, D. Xu, W. Yang, J. Zhang, *Food and Bioprocess Technology*, 13 (2020), 522-532. <https://doi.org/10.1007/s11947-020-02409-w>.
- [4] P. Díaz-Calderón, L. Caballero, F. Melo, J. Enrione, Molecular configuration of gelatin–water suspensions at low concentration, *Food Hydrocoll.* 39 (2014) 171-79. <https://doi.org/10.1016/j.foodhyd.2013.12.019>.
- [5] Q. Xing, K. Yates, C. Vogt, Z. Qian, M.C. Frost, F. Zhao, Increasing mechanical strength of gelatin hydrogels by divalent metal ion removal, *Sci. Rep.* 4 (2014) 1-10. <https://doi.org/10.1038/srep04706>.
- [6] H. Massoumi, J. Nourmohammadi, M.S. Marvi, F. Moztafzadeh, Comparative study of the properties of sericin-gelatin nanofibrous wound dressing containing halloysite nanotubes loaded with zinc and copper ions, *Int. J. Polym. Mater. Polym. Biomater.* 68 (2019) 1-12. <https://doi.org/10.1080/00914037.2018.1534115>.
- [7] W.W. Thein-Han, J. Saikhun, C. Pholpramoo, R.D.K. Misra, Y. Kitiyanant, Chitosan–gelatin scaffolds for tissue engineering: Physico-chemical properties and biological response of buffalo embryonic stem cells and transfectant of GFP–buffalo embryonic stem cells. *Acta Biomater.* 5 (2009) 3453-3466. <https://doi.org/10.1016/j.actbio.2009.05.012>.
- [8] X. Feng, V. K. Ng, M. Mikš-Krajnik, H. Yang, Effects of Fish Gelatin and Tea Polyphenol Coating on the Spoilage and Degradation of Myofibril in Fish Fillet During Cold Storage, *Food and Bioprocess Technology*, 10 (2017), 89-102. <https://doi.org/10.1007/s11947-016-1798-7>.
- [9] J. Rose, S. Pacelli, A. Haj, H. Dua, A. Hopkinson, L. White, F. Rose, Gelatin-based materials in ocular tissue engineering, *Materials* 7 (2014) 7, 3106-3135. <https://doi.org/10.3390/ma7043106>.
- [10] J.R. Dias, S. Baptista-Silva, C.M. Oliveira, A. de Sousa, A.L. Oliveira, P.J. Bartolo, P.L. Granja, In-situ crosslinked electrospun gelatin nanofibers for skin regeneration, *Eur. Polym. J.* 95 (2017) 161-173. <https://doi.org/10.1016/j.eurpolymj.2017.08.015>.
- [11] M. S. Rahman, G. S. Al-Saidi, N. Guizani, Thermal characterisation of gelatin extracted from yellowfin tuna skin and commercial mammalian gelatin, *Food Chemistry* 108 (2008) 472-481. <https://doi.org/10.1016/j.foodchem.2007.10.079>.
- [12] A. Duconseille, T. Astruc, N. Quintana, F. Meersman, V. Sante-Lhoutellier, Gelatin structure and composition linked to hard capsule dissolution: A review, *Food Hydrocoll.* 43 (2015) 360-376. <https://doi.org/10.1016/j.foodhyd.2014.06.006>.

- [13] E. Jeevithan, Z. Qingbo, B. Bao, W. Wu, Biomedical and Pharmaceutical Application of Fish Collagen and Gelatin: A Review, *Journal of Nutritional Therapeutics*, 2 (2013), 218-227.
- [14] A. Etxabide, I. Leceta, S. Cabezudo, P. Guerrero, K. de la Caba, Sustainable fish gelatin films: From food processing waste to compost, *ACS Sustainable Chem. Eng.* 4 (2016) 4626-4634. <https://doi.org/10.1021/acssuschemeng.6b00750>.
- [15] A. Mannu, S. Garroni, J. Ibanez Porras, A. Mele, Available technologies and materials for waste cooking oil recycling, *Processes* 8 (2020) 366. <https://doi.org/10.3390/pr8030366>.
- [16] M. Bocqué, C. Voirin, V. Lapinte, S. Caillol, J.J. Robin, Petrobased and bio-based plasticizers: Chemical structures to plasticizing properties. *J. Polym. Sci., Part A: Polym. Chem.* 54 (2016) 11-33. <https://doi.org/10.1002/pola.27917>.
- [17] A.A. Karim, R. Bhat, Fish gelatin: properties, challenges, and prospects as an alternative to mammalian gelatins, *Food Hydrocoll.* 23 (2009) 563-579. <https://doi.org/10.1016/j.foodhyd.2008.07.002>.
- [18] M. Ramos, A. Valdés, A. Beltrán, M.C. Garrigós, Gelatin-based films and coatings for food packaging applications, *Coatings* 6 (2016) 41. <https://doi.org/10.3390/coatings6040041>.
- [19] P.K. Binsi, N. Nayak, P.C. Sarkar, C.G. Joshy, G. Ninan, C.N. Ravishankar, Gelation and thermal characteristics of microwave extracted fish gelatin-natural gum composite gels, *J. Food Sci. Technol.* 54 (2017) 518-530. <https://doi.org/10.1007/s13197-017-2496-9>.
- [20] Y. Wu, W. Ding, L. Jia, Q. He, The rheological properties of tara gum (*Caesalpinia spinosa*), *Food Chemistry* 168 (2015) 366-371. <https://doi.org/10.1016/j.foodchem.2014.07.083>.
- [21] A. Mortensen, F. Aguilar, R. Crebelli, A. Di Domenico, M. J. Frutos, P. Galtier, D. Gott, U. Gundert-Remy, C. Lambré, J.-C. Leblanc, O. Lindtner, P. Moldeus, P. Mosesso, A. Oskarsson, D. Parent-Massin, I. Stankovic, I. Waalkens-Berendsen, R. A. Woutersen, M. Wright, M. Younes, L. Brimer, A. Christodoulidou, F. Lodi, A. Tard, B. Dusemund, Re-evaluation of tara gum (E 417) as a food additive, *EFSA Journal*, 15, 6 (2017), e04863. <https://doi.org/10.2903/j.efsa.2017.4863>.
- [22] Available online at: http://www.lapigelatine.com/wp-content/uploads/2017/01/fish.gelatine.edible.grade_.pdf (accessed on 10/10/2020).
- [23] J. Chong, O. Soufan, C. Li, I. Caraus, S. Li, G. Bourque, D.S. Wishart, J. Xia, MetaboAnalyst 4.0: towards more transparent and integrative metabolomics analysis, *Nucl. Acids Res.* 46 (2018) 486-494. <https://doi.org/10.1093/nar/gky310>.
- [24] F. Delogu, G. Gorrasi, A. Sorrentino. Fabrication of polymer nanocomposites via ball milling: Present status and future perspectives, *Prog. Mater. Sci.* 86 (2017) 75-126. <https://doi.org/10.1016/j.pmatsci.2017.01.003>.
- [25] B. S. Pascual, M. Trigo-López, J. A. Reglero Ruiz, J. L. Pablos, J. C. Bertolín, C. Represa, J. V. Cuevas, Félix C. García, J. M. García, Porous aromatic polyamides the easy and green way, *European Polymer Journal*, 116 (2019), 91-98. <https://doi.org/10.1016/j.eurpolymj.2019.03.058>.

- [26] S. Basu, U.S. Shivhare, T.V. Singh, V.S. Beniwal, Rheological, texture and spectral characteristics of sorbitol substituted mango jam, *J. Food Eng.* 105 (2011) 503-512. <https://doi.org/10.1016/j.jfoodeng.2011.03.014>.
- [27] UNE-EN 13432:2001 Requirements for packaging recoverable through composting and biodegradation. Test scheme and evaluation criteria for the final acceptance of packaging. 2001.
- [28] J. M. Chalmers, N. J. Everall, Polymer Analysis and Characterization by FTIR, FTIR-Microscopy, Raman Spectroscopy and Chemometrics, *Int. J. Polym. Anal. Charac.* 5 (1999), 223-245. <https://doi.org/10.1080/10236669908009739>.
- [29] M. S. Lindblad, B. M. Keyes, L. M. Gedvilas, T. G. Rials, S. S. Kelley, FTIR imaging coupled with multivariate analysis for study of initial diffusion of different solvents in cellulose acetate butyrate films, *Cellulose*, 15 (2008), 23-33. [Http://doi.org/10.1007/s10570-007-9173-5](http://doi.org/10.1007/s10570-007-9173-5).
- [30] B. Worley, R. Powers, Multivariate analysis in metabolomics, *Curr. Metabolomics* 1 (2013) 92-107. <https://doi.org/10.2174/2213235X11301010092>.
- [31] M.A. Meador, Recent advances in the development of processable high-temperature polymers. *Annu. Rev. Mater. Sci.* 28 (1998) 599-630. <https://doi.org/10.1146/annurev.matsci.28.1.599>.
- [32] E. Pulieri, V. Chiono, G. Ciardelli, G. Vozzi, A. Ahluwalia, C. Domenici, F. Vozzi, P. Giusti, Chitosan/gelatin blends for biomedical applications, *J. Biomed. Mater. Res. A.* 86 (2008) 311-322. <https://doi.org/10.1002/jbm.a.31492>.



Highlights:

- Novel films based on fish gelatin and tara gum were obtained.
- Films were fabricated following a simple casting process.
- Density of films varied between 6.5 and 9.8 g/cm³, using glycerol as plasticizer.
- High degradation temperatures (up to 300 °C) were observed.
- Milling Tara gum improved both thermal stability and mechanical strength.

Journal Pre-proof

Declaration of interests

The authors declare that they have no known competing financial interests or personal relationships that could have appeared to influence the work reported in this paper.

The authors declare the following financial interests/personal relationships which may be considered as potential competing interests:

Journal Pre-proof